

2018

Additive Manufacturing of Heat Exchangers

Jake Boxleitner

University of Wisconsin - Madison, United States of America, boxleitner@wisc.edu

Gregory F. Nellis

University of Wisconsin, United States of America, gfnellis@engr.wisc.edu

Follow this and additional works at: <https://docs.lib.purdue.edu/iracc>

Boxleitner, Jake and Nellis, Gregory F, "Additive Manufacturing of Heat Exchangers" (2018). *International Refrigeration and Air Conditioning Conference*. Paper 1919.

<https://docs.lib.purdue.edu/iracc/1919>

This document has been made available through Purdue e-Pubs, a service of the Purdue University Libraries. Please contact epubs@purdue.edu for additional information.

Complete proceedings may be acquired in print and on CD-ROM directly from the Ray W. Herrick Laboratories at <https://engineering.purdue.edu/Herrick/Events/orderlit.html>

Additive Design and Manufacturing of a Composite Polymer Heat Exchanger

Jake BOXLEITNER^{1*}, Gregory NELLIS²

^{1,2}University of Wisconsin - Madison,
Department of Mechanical Engineering,
Madison, WI 53706, United States of America
Email: ¹boxleitner@wisc.edu, ¹gfnellis@engr.wisc.edu

* Corresponding Author

ABSTRACT

The application of additive manufacturing to heat exchangers allows an unparalleled freedom in design. Fused Filament Fabrication (FFF) is a relatively low cost additive manufacturing process that involves depositing thermoplastic material layer by layer. The coupling of FFF with numerical models of air-side thermal fluid behavior has led to a novel, compact, high performance heat exchanger design that has been manufactured and validated experimentally. The heat exchanger features water and air in cross flow with various fin arrays on the air-side. Design paths towards cost and performance targets that will allow this technology to be competitive with industry targets have been identified and include: better understanding for manufacturing process constraints, filled material development, and air-side convection improvements.

In the FFF process, physical geometrical constraints such as extrusion nozzle diameter and layer height have implications on thermal performance, overall resistance to heat transfer, and manufacturability. Typical thermoplastic thermal conductivities are 100 to 1000 times smaller than that of the aluminum and copper used in industry standard heat exchangers. Efforts to manufacture polymers that are filled with conductive materials such as carbon fiber, aluminum flakes, and graphite aim to decrease this gap by an order of magnitude. To be competitive with traditional air-cooled heat exchangers with material that is much less conductive, air-side convection optimization using Computational Fluid Dynamics (CFD) has been utilized to implement and validate advanced air-side geometries.

An FFF manufactured heat exchanger that is cost and performance competitive with traditionally manufactured heat exchangers will open the door to a future in air-cooled systems that currently does not exist. This technology will allow heat exchangers to become lighter and fit in a smaller envelope as well as result in rapid replacement, high customization, increased fouling resistance and provide other secondary advantages.

1. INTRODUCTION

The Advanced Research Project Agency (ARPA) includes the Advanced Research In Dry cooling (ARID) program. The objective of the ARID program is to develop technologies that allow power plants to achieve high thermal-to-electric energy conversion efficiency with zero net water consumption. The most direct method of achieving this goal is to improve the thermal efficiency of dry-cooled condensers by reducing the air-side thermal resistance without significantly increasing either the capital cost or the fan power required to operate these devices. One approach to this is the application of additive manufacturing to dry cooled condensers in order to obtain a low cost, high performance heat rejection system. Conversations with air-cooled heat exchanger manufacturers have resulted in aggressive cost targets that must be met in order to make this technology commercially viable in relevant first markets. A leading manufacturer of air-to-water heat exchangers has indicated that their “gold-standard” heat exchanger for HVAC&R applications achieves economic and thermal performance of approximately \$10/kW and 7 kW/kg, respectively. This represents the limit of state-of-the-art air-cooled system performance that is the product of a many decades of engineering research.

2. DESIGN AND MODELING

2.1 Geometry Definition

The additively manufactured cross-flow heat exchanger topology consists of two parts: a macrostructure and microstructure. The microstructure contains a water channel, an air channel with a finned array, and the walls that separate the channels. The macrostructure consists of a series of the microstructures repeated in each dimension in order to achieve some overall performance targets. As a baseline, an airfoil fin array will be considered on the airside and the heat exchanger will be manufactured using a commercially available carbon fiber nylon filled filament, referred to as Onyx (Felber, 2017). The micro and macro structures are outlined in Figure 1.

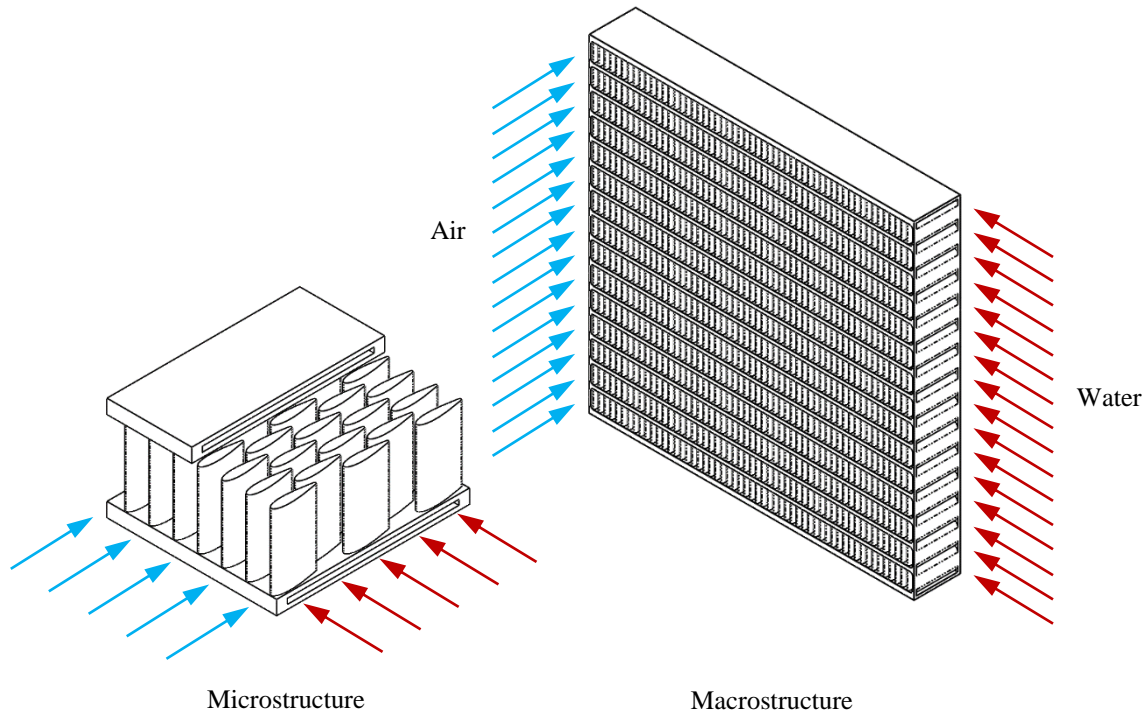


Figure 1: Cross-flow heat exchanger microstructure and macrostructure configuration

To predict and define the optimal geometry, a thermal resistance network representing heat flow from the hot water to the cool air is used; as shown in Figure 2. This network in conjunction with the ϵ -NTU method is used for determining the heat transfer rate in the macrostructure heat exchanger (Nellis, 2009). In traditional air-cooled heat

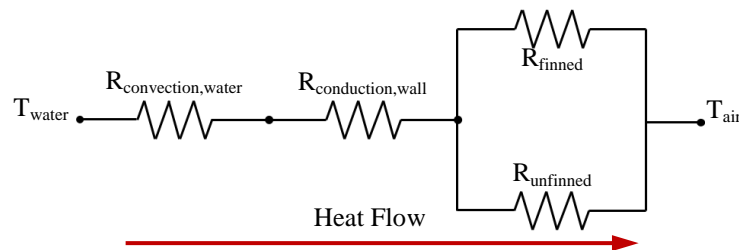


Figure 2: Thermal resistance network

exchangers, airside convection resistance is the limiting factor due to the low density of the fluid. In a polymer heat exchanger, performance is limited by airside convection but also by conduction resistances due to low thermal conductivity of the material. Because of these limiting factors, optimal geometries include small feature sizes and thin walls as small features yield high heat transfer coefficients and conduction resistance is highly dependent on

both wall thickness and conductivity. Thus, physical limits on geometries are set by manufacturing constraints like extrusion nozzle diameter and print layer height.

3. MANUFACTURING

3.1 Definitions and Nomenclature

In FFF printing, part print orientation is often such that the largest face area is placed in the x-y plane associated with the print bed and the shortest length is considered the z or build direction. This is done for both good adhesion to the build plate as well as to minimize print time and production costs. Figure 3 shows print orientation and build direction for an airfoil heat exchanger.

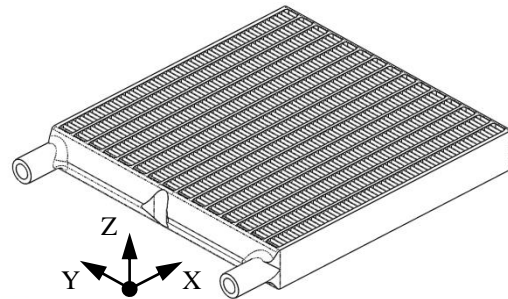


Figure 3: Heat exchanger build orientation – with headering

3.2 Tool Pathing

Before printing a complete heat exchanger, it is important to tune the process through a series of printing trials. These consist of initial printing of the airside geometry that allows quickly iterating through print parameters on a small test section of a microstructure. A challenge with printing the small features that exist on the airside is controlling movements of the tool head such that geometrical tolerances are met while depositing material as quickly as possible. The process of creating efficient layer-by-layer tool pathing is dependent on print parameters as well as how the geometry is modeled. Figure 4 shows the before and after of the initial slicer settings versus finalized settings that yield acceptable geometries.

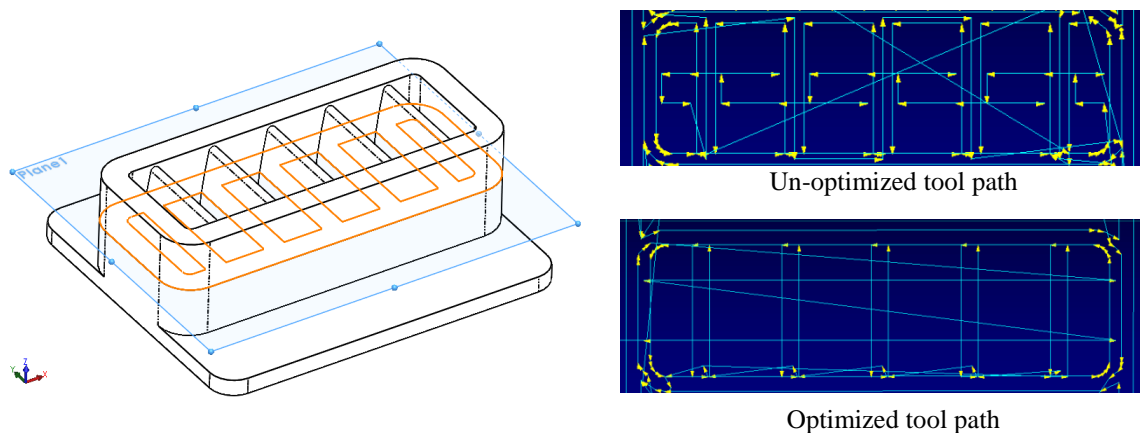


Figure 4: Left: sample microstructure geometry. Right: Un-optimized and optimized tool path for microstructure geometry at cut plane shown on left.

3.3 Geometric Inspection

As-printed microstructure geometries are inspected using Microcomputed Tomography or μ CT to enable high-resolution comparison to the as-modeled geometry. An example of this comparison is provided in Figure 5. In this

μ CT, image the extrusion nozzle and layer height that are defining characteristics of the FFF process visibly create a digital version of the modeled geometry. As previously mentioned, optimal geometries include small feature sizes and as the image shows there exists a trade-off between feature size and acceptable resolution of the as-printed geometry.

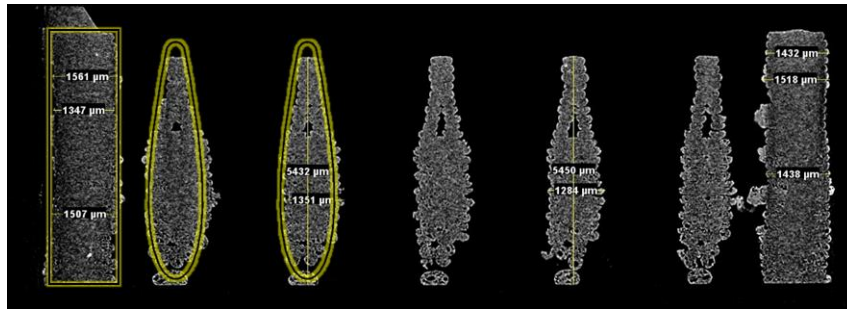


Figure 5: μ CT scan of sample microstructure

3.4 Water Tightness

After the proper print parameters have been identified that yield acceptable airside geometry, a microstructure including both air and water side geometry, referred to as a kazoo, is used to validate and identify print parameters that also yield water tight parts. The microstructure including water side geometry is shown in Figure 6.

Printing water tight channels can be a challenge and constrains the overall geometry that can be used. At every x-y location in every z plane, the weld created between layers must be uniform and each equally strong for a part to be operational. Through observation and a number of print setting studies, the parameters with greatest effects on water tightness have been identified as tool path, layer height, printing speed, extrusion multiplier, and temperature. Tool path is not a print parameter per se but rather a collective result related to how the geometry is modeled and how the slicer is being used to control print head movement. For every start, stop, and retraction the print head performs there is a discontinuity in the flow of material due to a delay before material flow reaches a consistent, steady state where it is likely to create a uniform weld between layers and thus a water tight part. For the remaining four parameters, a design of experiments was conducted to help identify the relationship each has in printing water tight kazoo parts. Burst or leak pressure was used as a quantifiable metric to characterize the water tightness; each kazoo was installed into a closed loop water system where the pressure of the loop was raised incrementally until the part failed.

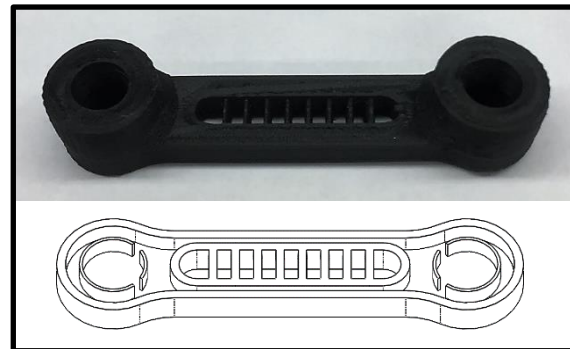


Figure 6: Top: as-printed kazoo. Bottom: kazoo cutaway showing internal water channels

It was concluded that geometries representative of this kazoo and more generally the intricate heat exchanger geometry required for this project must be printed at low layer heights, slow speeds, high extrusion ratios, and high temperatures. Low layer heights and slow speeds lead to increasingly longer print times which are an issue for both economic reasons as well as weld strength between layers for larger parts; both of which will be investigated at a later time.

In the study, two common failure modes were observed: the first at the interface of the fin and the wall, the second a sweating phenomenon that is visually analogous to a person breaking a sweat where the pressure pushes beads of water through the wall. The former is attributed to discontinuities in the tool path and the latter a result of poor weld strength and a bad combination of print parameters. Note that these results are somewhat geometry specific and therefore should be used as guideline to understand relationships. It is a strong, consistent weld at each layer that yields water tight parts and this is dependent on time between layers which is a result of tool path generation and print parameters specific to the material being used.

At this point, printing parameters that yield geometrically acceptable and water tight parts have been identified. Using these same parameters and tool pathing, a scaled down version of the heat exchanger is printed and used for testing and validating the thermal model.

4. EXPERIMENTAL VALIDATION

4.1 Heat Exchanger Testing

The experimental setup used to validate heat exchanger performance is modeled after the ASHRAE Standard 33 for testing air-cooling and heating coils. On the airside, these measurements include inlet temperature, outlet temperature, pressure differential across the heat exchanger, and pressure differential across a nozzle in the duct; the nozzle pressure differential is used to calculate air mass flow rate. On the waterside, these measurements include: inlet temperature, outlet temperature, pressure differential across the heat exchanger, and a mass flow measurement. Using the operating temperatures and flow rates scaled from the standard operating conditions provided by an industry source, the test section duct velocity is varied and all necessary measurements are taken to characterize the energy transfer for both fluids. Test results from the optimized airfoil geometry with the Onyx material are shown in Figure 7. The data is presented as mass-weighted performance (kW/kg) versus air side pressure drop (Pa). Mass-weighted performance is a metric used to capture thermal performance along with the mass used to construct the geometry; as mass is related to print time and cost of the heat exchanger. The figure demonstrates the agreement of energy transfer measurements between airside and water side fluids along with the thermal model used to determine the geometries.

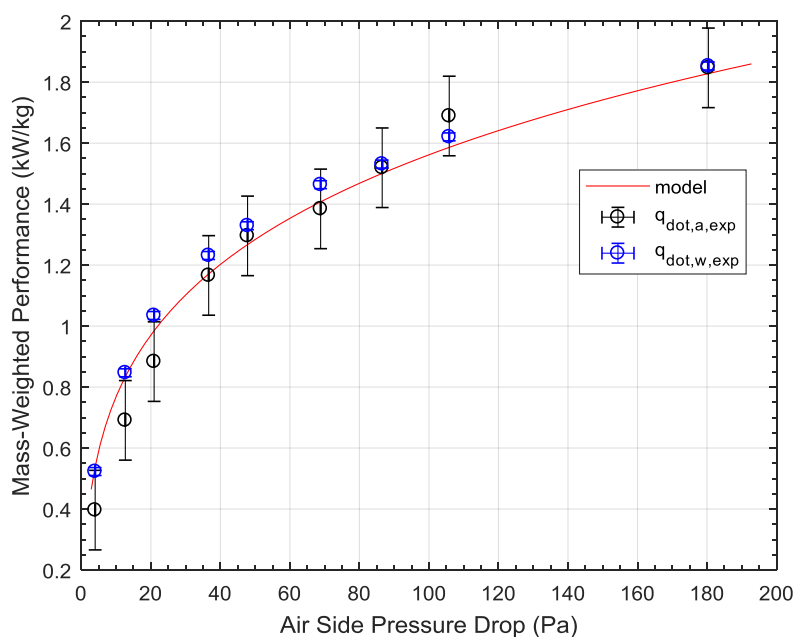


Figure 7: Baseline airfoil-Onyx geometry test results and thermal model prediction

4.2 Thermal Model Trade Studies

With a validated thermal model, it is appropriate to scale the geometry and run trade study scenarios to drive future design decisions to aid in reducing both airside convection resistance and conduction resistance. To motivate the subsequent section on material development, consider the conduction resistance and the two governing properties: thermal conductivity and wall thickness required to yield a water tight wall. Figure 8 presents the normalized performance of the heat exchanger as a function of material conductivity at two different wall thicknesses at optimized values of fin height and diameter. The figure demonstrates that an increase in thermal conductivity results in higher performance as conduction resistance in extended surfaces and through the wall decrease. It also shows that decreasing wall thickness has similar effects. In combination, if a neat polymer conductivity can be raised by an order of magnitude or more and water tight wall thickness can be printed at 0.8mm or less, there exists

diminishing returns on increased thermal conductivity as the limiting resistance to heat transfer is more heavily weighted towards airside convection.

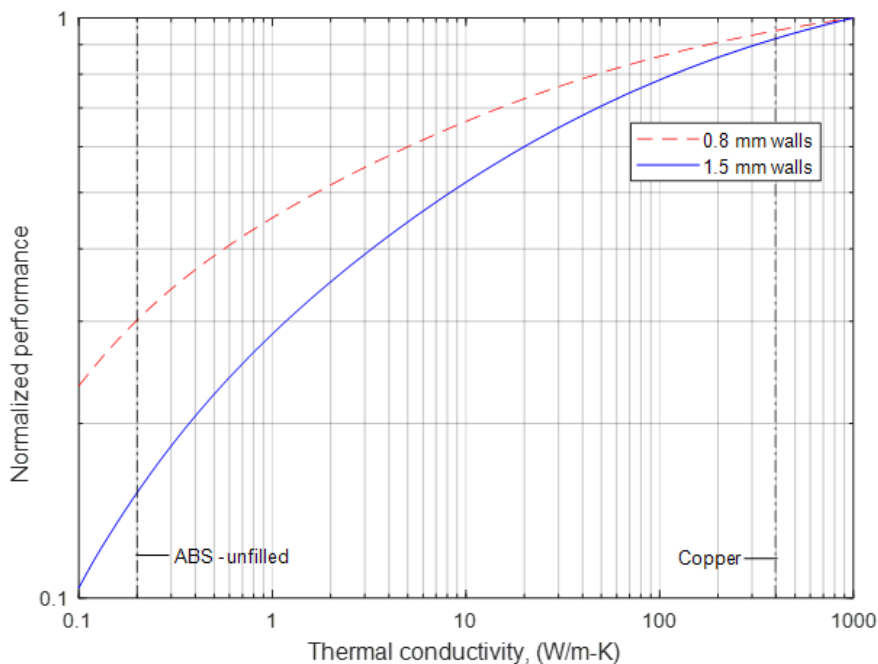


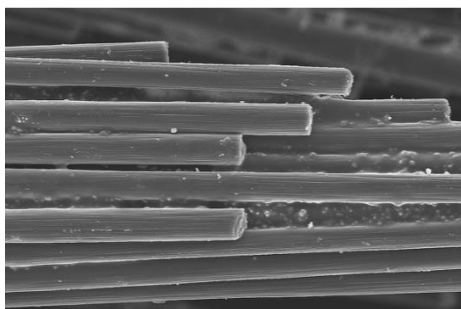
Figure 8: Thermal model predicted performance as a function of thermal conductivity.

5. MATERIAL DEVELOPMENT

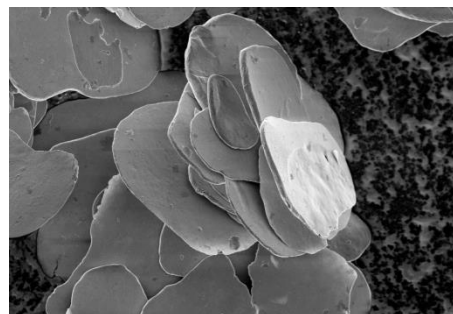
5.1 Filled Polymers

Typical neat-thermoplastic polymer thermal conductivities range from 0.1 – 0.3 W/m-K; however, to increase these conductivities fillers can be added to the base polymer. Common conductive fillers include copper, aluminum, graphite, carbon, etc. and come in an array of varying shapes: spheres, flakes, platelets, and fibers to name a few. When choosing a filler it is important to understand how the filler will be received by the base polymer as well as the implications this has on both the printability of the material and the effective thermal conductivity.

Flow-ability is a metric used to characterize how well a polymer matrix melt impregnated with a filler flows under printing conditions. As the volume percent of the filler increases, the flow-ability of the composite material decreases and thus there exists a limit to how much conductive filler you can add to the base polymer before it is unprintable. Another important decision to make when selecting a filler is filler shape. For example, two common



Carbon Fibers



Aluminum Flakes

Figure 9: Carbon fiber and aluminum flake S.E.M. images

filler types include flakes, and fibers: each have different implications on effective thermal conductivities within the heat exchanger due to FFF process dependent behaviors (Mulholland, 2017). To better understand these process dependent effects, a closer look at the fillers is needed. Figure 9 shows two Scanning Electron Microscope (SEM) images of short-strand carbon fiber and aluminum flake fillers. Due to the spaghetti-like shape of the carbon fibers, they exhibit high strength and high conductivity in the axial direction relative to the transverse directions resulting in a material with anisotropic properties. The aluminum flakes exhibit isotropic behavior in the two directions associated with the plane of the flake-like shape and anisotropic behavior in the remaining out-of-plane direction.

5.2 Filled Polymers in Printed Heat Exchangers

As these fillers exist in the filament and flow with the polymer melt through the extrusion nozzle, they preferentially orient with print direction. In Figure 10, a simple geometry showing tool path is used to demonstrate the alignment as well as establish a nomenclature for anisotropic thermal conductivity behaviors: conductivity in the print direction is referred to as k_1 , conductivity through adjacent bead lines in the same x-y plane is referred to as k_2 , and conductivity through adjacent bead lines in the build direction is referred to as k_3 . It should now be apparent that the printed part will have anisotropic thermal conductivity material properties specific to the tool pathing used to create the heat exchanger geometry.

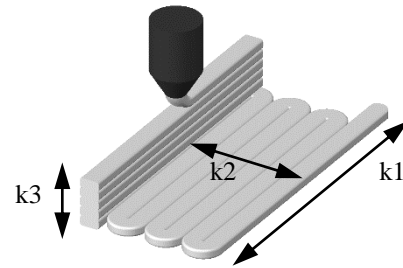


Figure 10: Generic conductivity orientation nomenclature

Conductivity k_1 is typically largest followed by k_2 and k_3 respectively with magnitude depending on filler type. Reconsidering the optimized tool path outlined in Figure 4 and the carbon fiber material: the high axial conductivity is aligned axially with the airfoil fins and the lower transverse conductivity governs the conduction resistance through the wall. To illustrate this, Figure 11 shows this tool pathing plane and the orientations of each conductivity value in the x-y plane. Optimally, a high conductivity is desired for both the extended surfaces as well as the transverse direction associated with conduction through the wall. For this reason, the aluminum flake is ideal as material properties are nearly isotropic in the x-y plane.

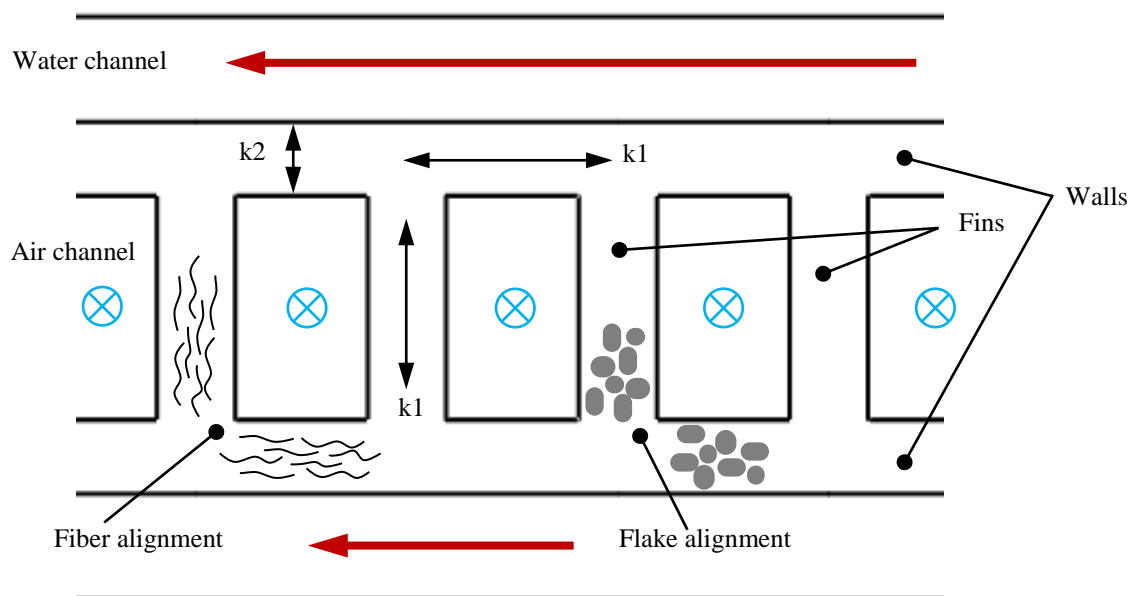


Figure 11: Tool path dependent conductivity orientations and filler alignment

6. GEOMETRY DEVELOPMENT

6.1 Tapered Pin Fins

As material development aims to increase thermal conductivity by an order of magnitude and process parameters aim to reduce wall thickness, airside convection increasingly becomes the limiting factor to performance. Tapered pin fins were examined through the use of CFD and found to yield substantially more heat transfer at lower pressure drop relative to standard pin fins as well as airfoil fins (Leeds, 2018). This is related to several, simultaneous improvements: the tapered fins have a higher heat transfer coefficient due to the lower average diameter, the fin efficiency (relative to the use of mass) is much higher as the material is placed in regions where conduction is highest, and the pressure drop is lower because of the larger open area for air flow. This geometry is outlined in Figure 12 and oriented with respect to the microstructure.

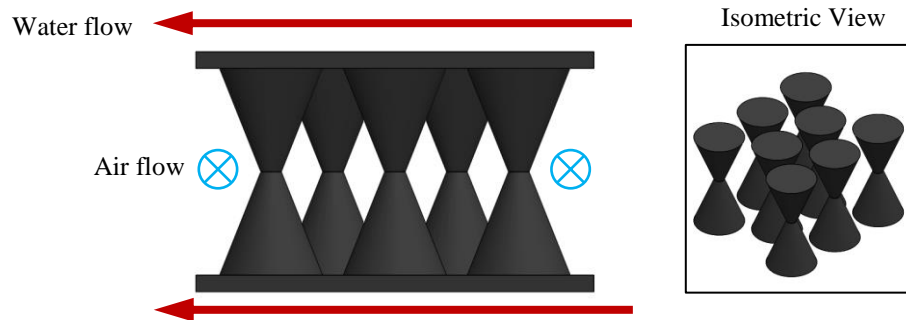


Figure 12: Tapered pin fin configuration

6.2 Manufacturing

Using similar processes and considerations as previously described for the airfoil fins process dependent limitations on the geometry exist. Also, as the kazoo design of experiments suggests, it is advantageous to manufacture these tapered fins with a continuous tool path around the perimeter of the fin then come back to fill in the base. As observed when manufacturing airfoil fins, failure modes primarily exist near regions of discontinuous tool pathing and this approach reduces wall discontinuity to one time per layer (rather than one time per fin).

To outline the process of slicing and controlling tool pathing for tapered fins, consider the single tapered fin shown in Figure 13 (Left) and three cut planes in the build direction: Layer A near the base of the fin, Layer C at

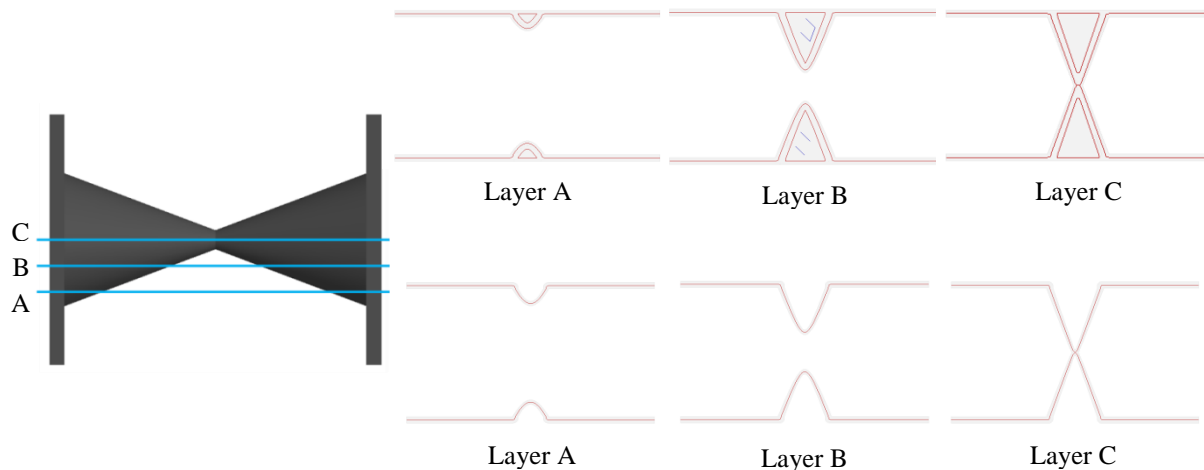


Figure 13: Left: Tapered pin fin tool path cut plane. Top: Initial tool path with infill. Bottom: Optimized tool path with no infill

the center of the fin, and Layer B at an intermediate distance between Layer A and Layer C. Considering cut plane Layers A, B, and C, tool pathing for this single tapered fin shown at the top of the figure. Observed in Layer A, the tool head “bumps” out from the wall creating the base of the fin, this bump is small enough that the material welds well to the previous layer but large enough such that it provides Layer B with enough support to create a larger bump in the following layers. After the initial perimeter of material geometrical establishes the fin, the tool head then comes back to fill in the fin base (if a solid fin is desired). This behavior continues, material growing out from the top and bottom walls until eventually a fin is formed, as observed in Layer C. From Layer C onwards, tool pathing is a mirror image of the previous layers. After observation of the tool pathing outlined, removing the tapered fin infill makes sense for both heat transfer and mass purposes; resulting in the tool pathing outlined at the bottom of the figure.

Now instead of a single tapered fin, consider the microstructure channel of six tapered fins shown in Figure 14; this channel is representative of a single air channel in a full scale heat exchanger. From a process and material perspective, the entire airside structure is now created in one continuous loop in every x-y plane of the build direction which results in quicker print times as there is no wasted movement associated with creating the geometry.

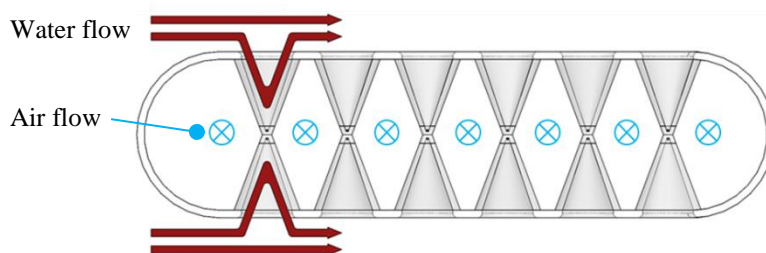


Figure 14: Tapered pin fin channel microstructure channel

There is less material usage as the base of the pins are hollow, and there exists a higher success rate for water tight parts: kazoo testing for the tapered pin fin geometry yielded no common modes of failure. From a heat transfer and water side hydraulic performance perspective, the geometry is no longer limited by extended surface conduction resistance as the water is able to flow into and shear out of the fin base resulting in a fin efficiency approaching unity. CFD studies were conducted on water side behavior in the fin bases and a relationship was found for the geometric aspect ratio and the presence of a water side thermal gradient due to stagnant, trapped water in the hollow fins. Results from this study helped put limits physical ranges and limits on the geometry that were then used to thermal model this problem.

Observation of this geometry and water side behavior suggests additional design modifications should allow/encourage water to flow through the fins. Creating structures like this involve an entirely different formulation of tool pathing and description of hydraulic behavior; discussion will be saved for another time.

6.3 Experimental Validation

Using the tapered pin geometry shown in Figures 12, 13, and 14 along with the manufacturing process previously developed, a tapered pin fin heat exchanger was modeled, printed using Onyx, and tested for model validation. Results are shown in Figure 15 and compared to the previous airfoil heat exchanger. For comparable air side pressure drop, the hollow-tapered fins outperform the airfoil geometry on a mass-weighted performance basis by nearly four times and performance approaches the initial goal of 7 kW/kg

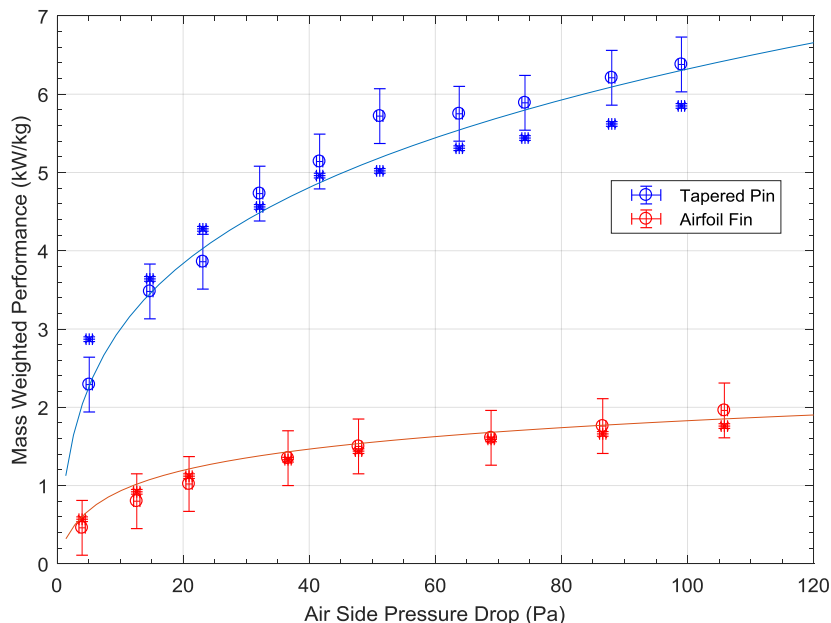


Figure 15: Tapered pin fin test results and thermal model comparison to airfoil results presented in Figure 7.

7. CONCLUSIONS

The combination of heat exchanger geometry and material development has proven that the FFF process is capable of manufacturing intricate geometries that are competitive with industry standards: the hollow tapered pin fin geometry and the aluminum flake heat exchanger mass-weighted performance is expected to exceed 8 kW/kg at an expected cost of \$13/kW. Future efforts will focus on continued geometry and material development as well as scaling and long-term reliability as the idea that this process has the potential to change the air-cooled heat exchanger industry with its unmatched degrees of freedom in design and manufacturing.

REFERENCES

- Felber, R., "Design, simulation, and testing of novel air-cooled heat exchangers manufactured by fused filament fabrication," M.S. thesis, Dept. of Mech. Eng., Univ. of Wisc., Madison, WI, 2017.
- Nellis, G.F., and Klein, S.A., Heat Transfer, 1st ed. New York, NY: Cambridge Univ. Press, 2009.
- Mulholland, T., et al. (2017). Journal of Materials, "Fiber Orientation Effects in Fused Filament Fabrication of Air-Cooled Heat Exchangers"
- Leeds, C., "Simulation of Tapered Pin Fins and Cylinders in Crossflow," M.S. thesis, Dept. of Mech. Eng., Univ. of Wisc., Madison, WI, 2018.

ACKNOWLEDGEMENT

The information, data, or work presented herein was funded in part by the Advanced Research Projects Agency-Energy (ARPA-E), U.S. Department of Energy, under Award Number DE-AR0000573. The views and opinions of authors expressed herein do not necessarily state or reflect those of the United States Government or any agency thereof.